Journal Name

COMMUNICATION

Target profiling of zerumbone using a novel cell-permeable clickable probe and quantitative chemical proteomics

Karunakaran A. Kalesh,[a] James A. Clulow [a] and Edward W. Tate[a*]

Zerumbone is a phytochemical with diverse biological activities ranging from anti-inflammatory to anti-cancer properties; however, to date the cellular targets of this important compound have remained elusive. Here we report the global protein target spectrum of zerumbone in living cancer cells using competitive activity-based protein profiling of a novel cell-permeable clickable probe, combined with quantitative mass spectrometry.

Zerumbone, (2,6,9,9-tetramethyl-[2E,6E,10E]-cycloundeca-2,6,10-trien-1-one), is a cyclic sesquiterpene isolated from the tropical plant *Zingiber zerumbet* Smith. Many *in vitro* and *in vivo* studies have indicated anti-cancer, anti-inflammatory and cellular detoxification properties for the compound,[1] however, the protein targets that may underlie these activities are yet to be characterised. The unusual cyclic α,β-unsaturated ketone functionality in the molecule (Fig. 1a) has been found to be essential for activity as it provides electrophilic Michael addition centres for irreversible covalent binding of target proteins via nucleophilic residues.[2] Zerumbone-bound sepharose gel and a biotinylated zerumbone derivative have been reported as biochemical tools for target profiling of this important bioactive compound,[3] but are of limited use in determining targets in living cells since these probe designs preclude representative cell-based experiments. We therefore designed a cell-permeable clickable probe and report herein the application of this probe in intact cells revealing, for the first time, the broad target spectrum of zerumbone using quantitative mass spectrometry-based chemical proteomics. Clickable small-molecule probes have been instrumental in target and off-target profiling of many drugs and biologically active natural products.[4] In order to elucidate the target spectrum of zerumbone we designed and synthesised the terminal alkyne incorporated zerumbone derivative **Yn-Zer** (Fig. 1a and ESI† Scheme 1) that places the tag distal to the key reactive centres in **Zer** (Fig. 1b).
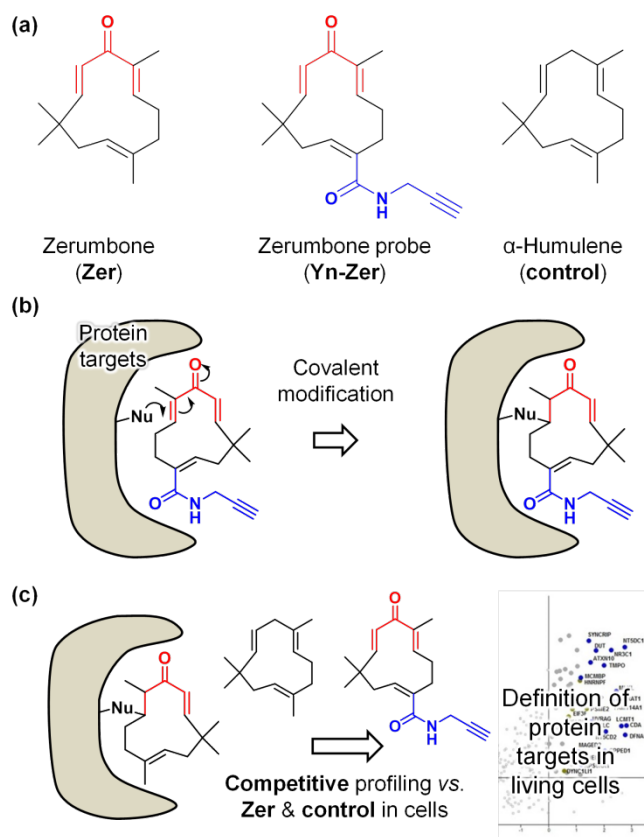

Fig. 1 (a) Structures of zerumbone (**Zer**), probe (**Yn-Zer**) and inactive zerumbone derivative α-humulene. (b) A potential mechanism of addition between nucleophilic target protein residues (**Nu**) and **Yn-Zer**. c) Competitive profiling against **Yn-Zer** in cells leads to targets of **Zer**.
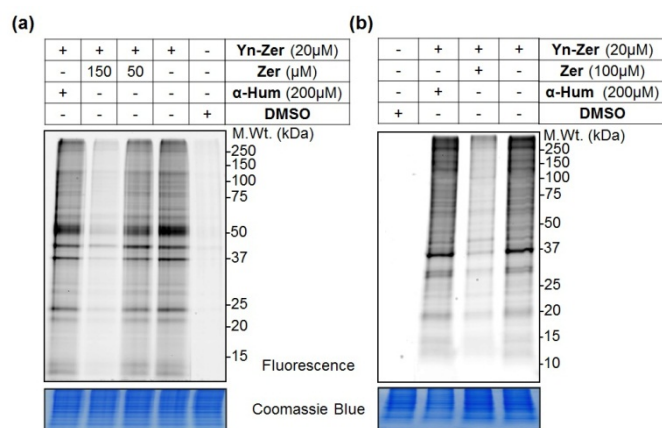
Fig. 2 In-gel fluorescence imaging of Yn-Zer-labelled HeLa proteome. (a) Lysate based labelling. (b) Intact cell-based labelling.

The probe design includes an α,β-unsaturated amide that is relatively much less reactive than ketone-conjugated alkenes such as those required for activity in **Zer**. We anticipated that any interference in target profiling would be factored out during quantitative analyses in cells (Fig. 1c), which depend on competition of **Zer** against **Yn-Zer**, rather than on identification of the probe targets themselves. Initial gel-based labelling experiments were carried out using HeLa whole cell lysates. The probe-treated lysate was subjected to copper catalysed azide-alkyne cycloaddition reaction (CuAAC) using a trifunctional capture reagent azido-TAMRA-biotin (AzTB) previously developed in our lab (see ESI†).[5] Proteome labelling was evaluated by in-gel fluorescence scanning following SDS-PAGE (Fig.2a). Multiple protein bands were labelled by the probe, and these were readily outcompeted with excess zerumbone. However, competition against α-humulene, a zerumbone derivative that lacks the reactive ketone functionality (Fig. 1a), showed no effect on labelling efficiency. This underlines the importance of the α,β-unsaturated ketone functionality in the protein reactivity of the probe and the parent compound, and suggests that the unsaturated amide
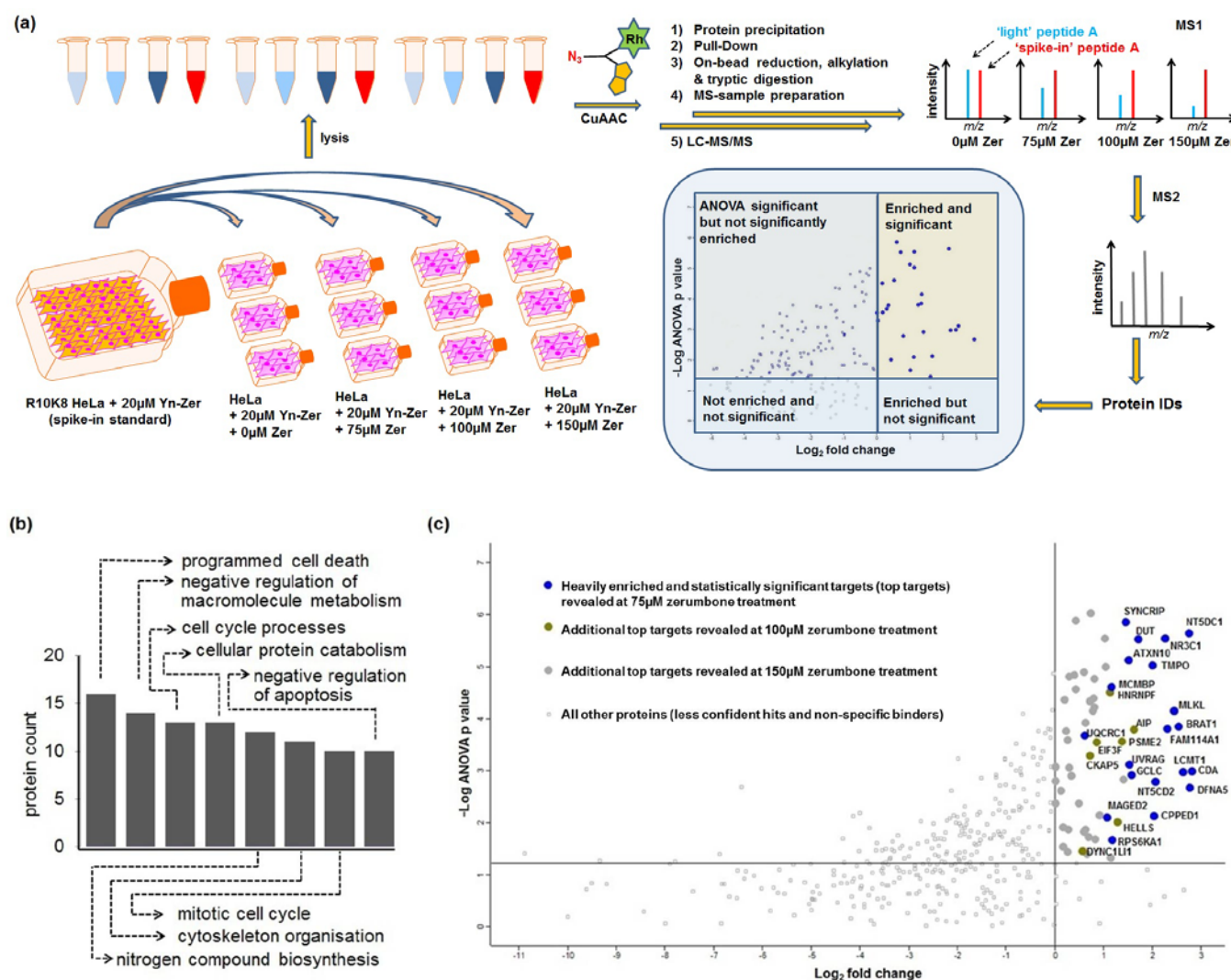
Fig. 3 (a) Overview of 'spike-in'-SILAC-coupled quantitative chemical proteomics methodology. (b) Key biological processes affected by zerumbone treatment revealed by DAVID bioinformatic analysis of 151 zerumbone-competed protein IDs. (c) Log2 fold change in the H/L ratios of identified hits upon zerumbone treatment vs. no zerumbone treatment as a function of statistical significance (-Log ANOVA p value) across the three biological replicates. The variance tested was the variance of means of H/L ratios of each protein across the three biological replicates. Top targets identified at 75µM and 100µM zerumbone are labelled (gene names) on the plot.

gene symbol	localisation	major protein functions
DFNA5	cytoplasm	apoptosis, cancer and cell survival.
CDA	cytoplasm, nucleus	scavenges cytidine and 2'-deoxycytidine for UMP synthesis
UVRAG	endosome, lysosome	DNA repair, positive regulation of autophagy, regulation of intrinsic pathway of apoptosis
LCMT1	cytoplasm	c-terminal protein methylation, regulation of apoptosis
NT5DC1	cytosol	hydrolase
CPPED1	cytoplasm	protein phosphatase of Akt-family kinases, blocks cell cycle progression and promotes apoptosis
NT5CD2	mitochondrion	hydrolase
FAM114A1	cytoplasm	neuronal cell development
GCLC	cytoplasm, cytosol	glutathione biosynthesis, cell redox homeostasis, apoptotic mitochondrial changes
MLKL	cell membrane, cytoplasm	TNF-induced necroptosis
NR3C1	cytoplasm, mitochondrion, nucleus	transcription regulation, affects inflammatory responses and cellular proliferation
ATXN10	cytoplasm	necessary for the survival of cerebellar neurons, apoptosis
TMPO	nucleus	regulation of transcription
RPS6KA1	nucleus, cytoplasm	serine/threonine kinase that regulate many cellular processes including growth, motility, survival and proliferation.
BRAT1	nucleus	cellular response to DNA damage
MCMBP	nucleus	cell cycle, cell division, DNA replication, mitosis
MAGED2	cytosol, nucleus	tumor antigen, protects melanoma cells from apoptosis induced by TRAIL
UQCRC1	mitochondrion	electron transport
SYNCRIP	cytoplasm, ER, microsome, nucleus, spliceosome	translation regulation, mRNA processing and splicing, host-virus interaction
DUT	mitochondrion, nucleus	nucleotide metabolism

Table 1 Top 20 targets of zerumbone revealed in this study.

in **Yn-Zer** does not significantly influence labelling.

We next investigated intact cell-based labelling using **Yn-Zer**. HeLa cells gown in DMEM medium pre-incubated with zerumbone or α-humulene (or DMSO as a vehicle control) for 30 min were treated with **Yn-Zer**. The cells were then washed with PBS, lysed and the lysates subjected to CuAAC ligation to AzTB followed by protein resolution on SDS-PAGE and in-gel fluorescence scanning (Fig. 2b). Labelling of several cellular proteins was observed and as in the case of the lysate-based experiment only the parent compound outcompeted proteome labelling by the probe, with α-humulene displaying no detectable effect. A comparison of the lysate- and cell-based experiments revealed significantly different labelling patterns, highlighting the importance of intact cell-based labelling for validation of physiologically relevant targets, which is a particular advantage of the current probe design.

Encouraged by the results from gel-based labelling, we performed large-scale proteomic experiments using a combination of probe labelling and Stable Isotope Labelling by Amino acids in Cell culture (SILAC)-based quantitative mass spectrometry (MS).[6] A 'spike-in' SILAC approach[7] (Fig. 3a), as recently implemented for human *N*-myristoyltransferase (NMT) substrate discovery,[8] was envisaged for global profiling of zerumbone targets as this method

enables an unbiased, high-confidence approach to target identification directly in the native cellular environment (i.e. at endogenous expression level and native protein folding). Spike-in SILAC methodology normalises all experimental samples across all sample handling steps and since heavy isotope labelling is required only for the 'spike-in'-standard, the experimental samples and the system under investigation are free from any potential disruption from isotope labelling or use of particular media. Briefly, HeLa cells cultured in normal DMEM media were treated separately in triplicate with 20μM **Yn-Zer** alone or with 20μM **Yn-Zer** in combination with three different concentrations (75, 100 and 150μM respectively) of zerumbone. In parallel, HeLa cells labelled with $^{15}N_4{}^{13}C_6$-arginine and $^{15}N_2{}^{13}C_6$-lysine (R10K8 HeLa cells) cultured and maintained in R10K8 DMEM media were treated with 20μM **Yn-Zer** to generate the 'spike-in' SILAC standard. After compound incubation cells were lysed, and lysate protein concentrations normalised across all samples. Heavy lysates were spiked into each sample in a 1:1 ratio, and the mixture subjected to CuAAC reaction with AzTB, as described above. The samples, after protein precipitation to remove capture reagent excess, were re-dissolved in protein buffer and subjected to affinity purification on NeutrAvidin-Agarose resin, followed by nanoLC-MS/MS proteomic analysis and data processing as described in the ESI.

A stringent cut-off threshold of at least 6 valid quantifications across the 12 samples for each protein led to identification of >600 proteins (ESI Supporting Table 1). Of these identified hits, 151 proteins displayed concentration-dependent competition against the parent compound (blue in ESI Supporting Table 1), suggesting that they are genuine cellular targets of the phytochemical. The high reproducibility of the data is clearly evident from the scatter plots displaying nearly linear relationship (ESI† Fig. S3) between H/L ratios of the majority of identified protein targets across the three biological replicates of each tested concentration of the parent compound. Multiple unique peptides (often 7 or more at a stringent false discovery rate of <1%) were identified for each protein target across the proteomic samples, along with high protein sequence and unique sequence coverage (ESI Supporting Table 1). The capability to assign rigorous and robust identity and quantification from multiple unique peptide data points during competition experiments highlights the advantages of MS/MS-based quantitative chemical proteomics in complex systems. Furthermore, the competition-based 'spike-in' SILAC methodology factors out any interference that might result from the conjugated amide in **Yn-Zer**.

Bioinformatic analysis of the zerumbone-competed proteome (151 protein IDs) using the Database for Annotation, Visualization and Integrated Discovery (DAVID) bioinformatics resource[9] revealed several specific key biological processes (Fig. 3b, ESI† Supporting Table 4) and biological pathways (ESI† Fig S1 & Supporting Table 3) that are targeted by zerumbone. In order to identify the most significantly engaged targets we plotted Analysis of Variance (ANOVA) significance (-log ANOVA p values) of all identified proteins as a function of fold change in enrichment following zerumbone treatment. As shown in Fig. 3a, proteins that are heavily enriched and significant will fall in the upper right quadrant and are high-confidence targets, whilst those in the lower right quadrant are also enriched but lack strong statistical significance, and thus represent lower-confidence targets. Proteins in the upper left quadrant, although statistically significant, are not strongly enriched, and those in the lower left quadrant are likely non-specific binders that are neither strongly enriched nor statistically significant. As shown in Fig. 3c, a total of 20 proteins (blue filled circles) displayed statistically significant enrichment at 75μM zerumbone, and with increasing concentration of competing zerumbone more protein targets are identified (7 additional targets at 100μM zerumbone and

35 additional targets at 150µM zerumbone). Table 1 lists the top 20 targets and their key biological functions (ESI† Supporting Table 2 lists the complete list of high-confidence targets and their key biological functions). The top targets of zerumbone are involved in vital biological processes, with many playing key roles in regulating apoptosis and cell survival. This multi-target activity of zerumbone demonstrated in this study strongly suggests that the compound exerts its biological effects via modulation of a variety of these targets in an interactome co-dependent and context-dependent manner.

Conclusions

In conclusion, we report the first large-scale profiling of zerumbone targets directly in live cancer cells using an integrated chemical proteomic approach that combines a cell-permeable small-molecule chemical probe with 'spike-in' SILAC-based quantitative proteomics. Using this methodology, the most potently engaged targets of the phytochemical could be determined in a concentration-dependent and high-throughput manner, in a native cellular environment. The data presented here provides valuable insights into molecular targets that potentially lead to the phenotypic changes and physiological effects observed following *in vitro* and *in vivo* administration of the phytochemical, and provide a basis for future biochemical studies to establish the mode of action of zerumbone. It is also important to note that many of the identified targets are implicated in diseases including cancers. Selective and potent inhibitors are not yet available for most of these targets, and this study could provide a starting point for inhibitor scaffolds against these proteins. Finally, as many biologically active natural products elicit their effects through multiple cellular targets rather than one single target, there may be physiologically and pathologically relevant co-dependencies across the identified targets and their interactome networks. For any given natural product, this network will require further investigation in order to reveal the complete molecular mechanisms behind their biological effects. Investigations in this direction for zerumbone are in progress in our group, and the results will be reported in due course.

Acknowledgements

Notes and references

a Department of Chemistry, Imperial College London, South Kensington Campus, Exhibition Road, London SW7 2AZ, UK, E-Mail: e.tate@imperial.ac.uk; Fax: +44 (0)20 7594 1139.

†Electronic Supplementary Information (ESI) available: Detailed experimental procedures and results.

1   R. Prasannan, K. A. Kalesh, M. K. Shanmugam, A. Nachiyappan, L. Ramachandran, A. H. Nguyen, A. P. Kumar, M. Lakshmanan, K. S. Ahn and G. Sethi, *Biochem. Pharmacol.*, 2012, **84**, 1268.

2   (a) S-H. Choi, Y-J Lee, W. D. Seo, H-J. Lee, J-W. Nam, Y. J. Lee, J. Kim, E-K. Seo and Y-S. Lee, *Int. J. Radiat. Oncol., Biol., Phys.*, 2011, **79**, 1196; (b) A. Murakami, D. Takahashi, T. Kinoshita, K. Koshimizu, H. W. Kim, A. Yoshihiro, Y. Nakamura, S. Jiwajinda, J. Terao and H. Ohigashi, *Carcinogenesis*, 2002, **23**, 795; (c) Y. Nakamura, C. Yoshida, A. Murakami, H. Ohigashi, T. Osawa and K. Uchida, *FEBS Lett.*, 2004, **572**, 245.

3   (a) K. Ohnishi, K. Irie and A. Murakami, *Biosci. Biotechnol. Biochem.*, 2009, **73**, 90265-1; (b) K. Ohnishi, S. Ohkura, E. Nakahata, A. Ishisaka, Y. Kawai, J. Terao, T. Mori, T. Ishii, T. Nakayama, N. Kioka, S. Matsumoto, Y. Ikeda, M. Akiyama, K. Irie and A. Murakami, *PLoS One*, 2013, **8**, e58641.

4   (a) Y. Su, J. Ge, B. Zhu, Y-G. Zheng, Q. Zhu and S. Q. Yao, *Curr. Opin. Chem. Biol.*, 2013, **17**, 768; (b) T. Böttcher, M. Pitscheider and S. A. Sieber, *Angew. Chem. Int. Ed.*, 2010, **49**, 2680; (c) P-Y. Yang, K. Liu, M. H. Ngai, M. J. Lear, M. R. Wenk and S. Q. Yao, *J. Am. Chem. Soc.*, 2010, **132**, 656; (d) H. Shi, C-J. Zhang, G. Y. J. Chen and S. Q. Yao, *J. Am. Chem. Soc.*, 2012, **134**, 3001.

5   (a) W. P. Heal, M. H. Wright, E. Thinon and E. W. Tate, *Nat. Protoc.*, 2012, **7**, 105; (b) M. H. Wright, B. Clough, M. D. Rackham, K. Rangachari, J. A. Brannigan, M. Grainger, D. K. Moss, A. R. Bottrill, W. P. Heal, M. Broncel, R. A. Serwa, D. Brady, D. J. Mann, R. J. Leatherbarrow, R. Tewari, A. J. Wilkinson, A. A. Holder and E. W. Tate, *Nat. Chem.*, 2014, **6**, 112.

6   (a) S-E. Ong, B. Blagoev, I. Kratchmarova, D. B. Kristensen, H. Steen, A. Pandey and M. Mann, *Mol. Cell. Proteomics*, 2002, **1**, 376; (b) M. Mann, *Nat. Rev. Mol. Cell. Biol.*, 2006, **7**, 952.

7   T. Geiger, J. R. Wisniewski, J. Cox, S. Zanivan, M. Kruger, Y. Ishihama and M. Mann, *Nat. Protoc.*, 2011, **6**, 147.

8   E. Thinon, R. A. Serwa, M. Broncel, J. A. Brannigan, U. Brassat, M. H. Wright, W. P. Heal, A. J. Wilkinson, D. J. Mann and E. W. Tate, *Nat. Commun.*, 2014, **5**, 4919.

9   (a) D. W. Huang, B. T. Sherman and R. A. Lempicki, *Nat. Protoc.*, 2009, **4**, 44; (b) D. W. Huang, B. T. Sherman and R. A. Lempicki, *Nucleic Acids Res.*, 2009, **37**, 1.

ChemComm Accepted Manuscript